HHS Public Access

Author manuscript

Lab Chip. Author manuscript; available in PMC 2018 March 29.

Published in final edited form as:

Lab Chip. 2017 March 29; 17(7): 1297–1305. doi:10.1039/c6lc01532h.

A Microfluidic Perfusion Approach for On-Chip Characterization of the Transport Properties of Human Oocytes

Prof. Gang Zhao,
Department of Electronic Science and Technology, University of Science and Technology of China. Hefei, Anhui 230027, China

Zhiguo Zhang,
Reproductive Medicine Center, Department of Obstetrics and Gynecology, The First Affiliated Hospital of Anhui Medical University, Hefei, Anhui 230022, China

Yuntian Zhang,
Department of Electronic Science and Technology, University of Science and Technology of China. Hefei, Anhui 230027, China

Zhongrong Chen,
Department of Electronic Science and Technology, University of Science and Technology of China. Hefei, Anhui 230027, China

Dan Niu,
Department of Electronic Science and Technology, University of Science and Technology of China. Hefei, Anhui 230027, China

Prof. Yunxia Cao, and
Reproductive Medicine Center, Department of Obstetrics and Gynecology, The First Affiliated Hospital of Anhui Medical University, Hefei, Anhui 230022, China

Prof. Xiaoming He
Department of Biomedical Engineering, The Ohio State University, Columbus, Ohio 43210, USA

Abstract

Accurate characterization of the cell membrane transport properties of human oocytes is of great significance to reproductive pharmacology, fertility preservation, and assisted reproduction. However, the commonly used manual method for quantifying the transport properties is associated with uncontrolled operator-to-operator and run-to-run variability. Here, we report a novel sandwich structured microfluidic device that can be readily fabricated for characterizing oocyte membrane transport properties. Owing to its capacity of excellent control of both solution replacement and temperature in the microchannel, the temperature-dependent permeability of oocyte membrane can be precisely characterized. Furthermore, the fertilization and developmental

Correspondence to: Gang Zhao.

(G. Zhao and Z. Zhang contributed equally to this work)

Author Contributions

GZ and XH conceived and designed the experiments, and analyzed data and wrote the manuscript. ZGZ, YTZ, ZRC, DN and YXC performed experiments. All authors commented on the manuscript.

competence analysis post perfusion indicate that our approach does not compromise the physiological function of in-vitro matured human oocytes. Collectively, we present the development of a novel sandwich structured microfluidic device based approach that allows for on-chip characterization of the transport properties of human oocytes under innocuous osmotic shock or injury to the cells.

Keywords

microfluidic perfusion chamber; cryopreservation; in vitro matured human oocytes; transport property; cell membrane permeability

Introduction

Oocyte transport properties refer to the temperature-dependent permeability of oocyte membrane to water (also known as hydraulic conductivity) and other small molecules that can be either cryoprotective agents or therapeutic drugs.[1–3] Accurate characterization of the cell membrane transport properties of human oocytes is of great significance to reproductive pharmacology, fertility preservation, and assisted reproduction.[4–7] For example, in the field of oocyte cryopreservation (a typical method for female fertility preservation), the success rate remains very low although there have been inspiring reports on the births achieved by fertilization of cryopreserved oocytes.[8] This is because the methods for oocyte cryopreservation are still suboptimal.[5, 9–13] A typical oocyte cryopreservation procedure includes addition/removal of cryoprotective agents (CPAs) and freeze-thaw cycles, which may put the cells at the risk of injuries caused by osmotic shock and extra-/intra-cellular ice formation.[14, 15] Quantitative understanding of cell responses upon such non-isotonic conditions and accurate measurement of the transport properties of the oocyte membrane are of considerable importance to the fields of oocyte cryopreservation.[16–19]

However, the commonly used method, manual pipetting (the micropipette perfusion[20–22] or the direct microscopic observation[2, 23–25] method), for quantifying the transport properties is associated with uncontrolled operator-to-operator and run-to-run variability.[3, 18] At the same time, the microscope diffusion chamber[26, 27] or the microperfusion chamber[28] has a comparatively complex structure (a dialysis or transparent porous membrane is introduced) that is hard to assemble.[29] Although microfluidic devices made of polydimethylsulfoxide (PDMS) have been used to investigate the cell membrane transport properties,[18, 19, 30, 31] the need of specialized facility including clean room for fabrication of the masks for soft lithography and a plasma cleaner for bonding, may not be readily available to many researchers. Moreover, the thermal/mechanical aging of PDMS makes microdevices made of PDMS alone unsuitable for long-term or repeated use.[32–35]

Here we report a novel microfluidic device that can be readily fabricated for characterizing the cell membrane transport properties. We demonstrate the feasibility and accuracy of the approach using *in vitro* matured human oocytes.

Materials and Methods

Design and fabrication of microfluidic device

As schematically illustrated in Figure 1A, the microdevice system mainly consists two parts: a temperature-controlled stage made from a plexiglas cuboid (120 × 70 × 10 mm, δ1=10 mm in thickness) and a microfluidic perfusion chamber with a silicone rubber gasket (δ2=1mm in thickness) clamped between them for sealing to prevent coolant leakage from the stage. The plexiglas cuboid has a milled cavity (80 × 30 × 9 mm) at the bottom for coolant flow. In the light of Takamatsu et al.'s work,[36] the microfluidic perfusion chamber was made by sandwiching two silicone rubber sheets (Kenis Limited, Osaka, Japan) between two silica glass slides (50 × 100 × 1.2 mm; δ3=δ6=1.2mm in thickness). The upper silicone rubber sheet (δ4=100 μm in thickness) with two identical cutouts (20 mm × 2 mm, 15 mm apart) and the lower sheet (δ5=50 μm in thickness) with one long cutout (55 mm × 2 mm) were aligned/overlapped and sandwiched between the two glass slides to form the microchannel that is 150 μm deep on both sides and 50 μm deep at the central area (inset i of Figure 1B). The height of the flow channel reduces from 150 to 50 μm at the uncut part between the two cutouts of the upper silicone rubber sheet (δ4) (Figure 1A), which enables trapping human oocytes (~100 μm in diameter) at the edge of the uncut part (inset ii of Figure 1B) for studying their membrane transport properties.

A narrow groove (5 × 0.8 × 0.3 mm) was slotted on the top surface of the bottom glass slide to allow placement of a tiny thermocouple (127 μm in diameter; TT-K-36, Omega Engineering, Inc., Stamford, USA) (Figure 1A). The thermocouple was connected to a data acquisition system (HP Agilent 34970A with 34901A module; Agilent, Santa Clara, CA, USA) for monitoring and recording temperature at the site where cells are trapped in the microfluidic channel.

Two holes (3 mm in diameter) were drilled in the upper glass slide as the inlet and outlet of the perfusion solution (Figure 1A and B). The inlet was connected to two syringes (S1 and S2: 5 ml, Figure 1B) using Teflon tubes and two Tee connections (inner diameter, 0.5 mm; outer diameter, 3 mm) for controlling the addition and removal of CPAs (in the hypertonic solution in syringe S2) with one of the Tee connections being open for cell loading. The outlet was connected to a syringe (S3: 5 ml) for collection of the used solution. The syringes were mounted on Legato 110P (KD Scientific Inc., Holliston, MA, USA) syringe pumps for controlled infusion/withdraw.

The components were tightly assembled with eight tiny clips and the assembled microdevice was mounted on the stage of an inverted microscope (CKX41, Olympus, Japan) equipped with a DP 71 CCD camera (Olympus, Tokyo, Japan) for video recording.

Chemicals and reagents

All reagents were purchased from Sigma-Aldrich (St. Louis, MO, USA) except where otherwise stated. Embryo culture medium, gonadotropin-releasing hormone antagonist (GnRHa), recombinant human follicle-stimulating hormone (r-hFSH), and human chorionic gonadotropin (hCG) were purchased from Cook Co. (Bloomington, IN, USA), Ipsen Pharma (Boulogne-Billancourt, France), Merck Serono Co. (Geneva, Switzerland), and Livzon

Pharmaceutical Group, Inc. (Zhuhai, China), respectively. The isotonic solution (268 ± 0 mOsm) was Quinns Advantage Medium with HEPES (In-Vitro Fertilization, Inc., Trumbull, CT, USA) and 10% v/v serum substitute supplement (IvineScientific, Santa Ana, CA, USA); the hypertonic solutions: 0.56 M Trehalose (981±1 mOsm), 1.5 M EG (2147±5 mOsm) and 1.5 M PG (2017±2 mOsm) in the isotonic solution. The osmolality of the perfusion solutions was measured using an osmometer (Model 3250, Advanced Instruments Inc., Norwood, MA, USA) in quintuplicate and the results are shown in Table S2 (Supplementary Information).

Isolation, in vitro maturation, fertilization of human oocytes and development of the fertilized oocytes

This project was approved by the ethical and scientific committee of the First Affiliated Hospital of Anhui Medical University, and written consent was obtained from all patients. Oocytes at the germinal vesicle (GV or MI) stage were obtained from the patients under the age of 35 who underwent ovarian stimulation using GnRHa protocol combined with rhFSH. The hCG injection was performed when the diameter of the leading ovarian follicle larger or equal to 18 mm, about 36 h later, oocyte retrieval was conducted by vaginal-ultrasound-guided puncture of ovarian follicles. Only high-quality GV and MI oocytes with appropriate size (~120 μm), normal zona pellucida, and integral membrane based on morphological evaluation under an inverted microscope (IX71, Olympus, Japan) were collected. The protocols for *in vitro* maturation (IVM), ICSI, and embryo culture are detailed elsewhere.[37] Briefly, GV or MI oocytes were cultured in self-prepared IVM medium supplemented with 75 mUI/ml r-FSH, 75 mIU/ml hCG and 20% patient serum[37, 38] with 6% CO_2 and 5% O_2 at 37 °C for 24 h. Matured oocytes at the stage of metaphase II, (MII) with visible 1st polar body and mitotic spindle as assessed under the inverted microscope were collected and inseminated by ICSI using sperm collected from the respective patients' husbands. The inseminated oocytes (both fresh control and perfused with a CPA addition-removal cycle) were cultured individually in cleavage medium droplet (30 μl) under mineral oil (300–400 μl) in 35 mm culture dish. Oocytes were observed for two pronuclei (2PN) formation at 16 h after ICSI. The embryo development was evaluated after another 24 h.

Oocyte perfusion, image acquisition and analysis

All the tubes and the microchannel were sterilized and filled with the isotonic solution, and then the experimental temperature was set by adjusting the temperature of the coolant *via* a cooling bath (NCB-2400, Eyela Tokyo Rikakikai Co., Ltd., Tokyo, Japan). The oocyte was gently drawn into a transfer tube using a 1 ml tuberculin syringe, and then manually infused into the microchannel through the open port for cell input (Figure 1B). Once the oocyte was successfully loaded, the cell input port was closed using a small clip and kept shut throughout the whole perfusion process.

Considering the fact that 0.5–1 M nonpenetrating (sucrose, trehalose, galatose, etc.) and 1–2M penetrating CPAs (dimethyl sulfoxide or DMSO, glycerol, EG, PG, etc.) are commonly used for cell cryopreservation by controlled cooling rate freezing,[15, 39, 40] osmotic responses of human oocytes upon 0.56 M Trehalose, 1.5 M EG, or 1.5 M PG in the isotonic solution were performed for investigation of oocyte membrane permeability as with most of previous

studies.[25, 41–46] The temperature dependence of the permeability (Arrhenius relationship[2, 47, 48]) is another essential part of the oocyte membrane transport properties, which requires the permeability data at least two different temperatures.[1] We chose three typical temperatures (4, 15, and 25 °C) for this study because almost all the studies on this topic used two to four different temperatures ranging over −3 to 37 °C,[25, 41–46, 49] 4 °C is the typical temperature commonly used for short-term preservation of biosamples, and 25 °C is the room temperature under which CPA loading/unloading is often done.

After 4 min of equilibration in the isotonic solution, the oocyte was exposed to a hypertonic solution (0.56 M Trehalose, 1.5 M EG, or 1.5 M PG in the isotonic solution) for 15–30 min, followed by an additional 20 min of isotonic perfusion. The injection speed of all the syringe pumps was set at 15 μL/min. The volume responses during the CPA addition-removal cycle were recorded using a DP 71 CCD camera (Olympus, Tokyo, Japan). The experiments were repeated for 6–10 times at each combination of temperature (4, 15, or 25 °C) and CPA concentration (0.56 M Trehalose, 1.5 M EG, or 1.5 M PG). Each oocyte was used for only once, and only one oocyte was loaded for each run to avoid mutual interference.

A series of image frames were extracted from the recorded video at 10 s of interval. The image processing software package ImageJ (V1.48, National Institutes of Health, Bethesda, USA) was used to measure the projected areas of the cells. The area values were then converted into volume assuming that the cells were spherical. The change in volume as a function of time was used to determine the cell membrane transport properties.

Results and Discussion

Osmolality distributions in the microchannel and extracellular osmolality profiles

The typical locations (P1, P2, and P3) of a cell in the microchannel are shown in inset iii of Figure 1B, where A1–A3 denote three different cross-sections at the front, middle, and rear of the cell. Taking P1 as an example, the osmolality distributions of solution on the cell surface and in the microchannel after introducing 0.56 M trehalose, 1.5 M ethylene glycol (EG), and 1.5 M propylene glycol (PG) at 25 °C were predicted using numerical models consisting of Eqs. (S1–S4) with necessary parameters listed in Table S1 and S2 (Supporting Information), and the results are shown in Figure S1. To comprehensively evaluate the mass transport, three times, t1, t2, and t3, were defined as the typical time to achieve 20, 50, and 80% of osmotic shift, respectively, from the initial value (0.268 Osm for an isotonic solution where the CPAs including trehalose, EG, and PG were dissolved) to the maximum osmolality. The average osmolality over cell surface over time, calculated using Eq. (S5) (Supporting Information), is shown in Figure S1 A–C. Being different from the assumption that the osmolality over the cell surface is homogeneous and the same as that of the introduced solution taken in most of the existing studies,[50–52] it takes time for the osmolality over the cell surface to reach that of the introduced solution. This characteristic time (Δt_c required for complete replacement of the initial isotonic (0.268 Osm) solution with the newly introduced hypertonic solution is similar for the three CPAs (27.3, 26.8, and 27.7 s for trehalose, EG, and PG, respectively, Figure S1 A–C). This similarity may be due to the fact that, for the given concentration and temperature, the diffusion coefficients of all the three CPA molecules in water are similar.[53–56] The transient osmolality distributions in the

microchannel (inset i of Figure 1B) and at the representative cross sections A1–A3 (insets ii and iii of Figure 1B) at the three characteristic times (t1–t3) are shown in Figure S1 D–F and G–I, respectively. The predictions for the locations P2 and P3 are shown in Figures S2 and S3, respectively. The results for P2 and P3 are similar to corresponding ones of P1, except that the characteristic times for CPA replacement are slightly longer at P3 than P1 and P2 with those at P1 being the shortest.

The average osmolality over cell surface (M_c, Osm) and the transient osmolality distributions at the typical time t2 (when M_c reached the average of the initial (M_i) and the maximum final (M_f) values, (M_i+M_f)/2) for both the cross section A2 (inset ii and iii of Figure 1B) and the cell surface are shown in Figure 2. The time-dependence of M_c at P1 and P2 is similar but faster than that at P3 (Figures 2 A–C). This is consistent with the fact that there is a pseudo-parabolic velocity field distribution of laminar flow in a microchannel with the no-slip boundary condition,[57, 58] and the velocity is faster in the area far away from the boundary than that near the boundary. The osmolality distributions for the cross section A2 (inset ii and iii of Figure 1B) and the cell surface (viewpoint along the flow direction) at the different t2 values of the different locations P1–P3 are shown in Figures 2D–F and G–I, respectively. It can be seen that the osmolality distribution over the cell surface is non-uniform, which indicates the importance of using the integral-averaged CPA concentration (Eq. S5, Supplementary Information) to quantify the cell membrane transport properties. Conventionally, step-wise input functions of extracellular osmolality profiles have been widely used in the two-parameter equations (Eqs. S6–S7, 2-*p* model) for describing the cell volume responses upon osmotic shift.[59–63] However, the extracellular osmolality over the cell surface in the microfluidic perfusion chamber changes gradually rather than step-wise. This gradual increase in extracellular osmolality is important for reducing sublethal cell injuries,[3] to ensure accurate measure of the membrane transport properties of healthy live cells.

Oocyte volume responses upon CPA replacement and determination of oocyte membrane transport properties

Representative photomicrographs showing the volume responses of typical *in-vitro* matured human oocytes to the addition of 0.56 M trehalose, 1.5 M EG, and 1.5 M PG at 25 °C are shown in Figure 3. The membrane transport properties of the oocyte were determined by nonlinearly fitting the 2-*p* model (Eqs. S6–S7, Supplementary Information) to the experimentally measured cell volume data. Representative cell volume responses and the corresponding curve-fitting results are shown in Figure 4A. The cells dehydrate with the addition of 0.56M trehalose that does not penetrate through the cell membrane, but they dehydrate first and then gradually rehydrate upon the addition of 1.5 M EG or PG that can enter the cells. The cell dehydration is caused by water outflow driven by the difference in the chemical potential of intra- and extracellular water, while the volume recovery was a result of the co-transport of water and CPA into the cell.[64–67] At the same time, the rate of cell dehydration and the extent of volume recovery reduce with decreasing temperature. The cell membrane permeability coefficients obtained by the aforementioned nonlinear cure-fitting method at various temperatures are listed in Table S3 (Supplementary Information), which also includes all the available data reported in previous studies on human

oocytes.[25, 27, 41–46] The results obtained in this study are within the range of data reported in the literature, suggesting the reliability of the new approach developed in this study.

To fully describe the transport properties of the cell membrane, both the reference values for the permeability coefficients at 0 °C (L_{pg} and P_{sg}) and the activation energies (E_{Lp} and E_{Ps}) that dictate their temperature dependence (see Eqs. S9 and S10) should be determined. Accordingly, the Arrhenius plots (see Eqs. S11 and S12) of both L_p and P_s versus 1/T are shown in Figure 4B. The values of L_{pg}, P_{sg}, E_{Lp} and E_{Ps} were determined based on the slopes and interceptions of the Arrhenius plots. The results (i.e., L_{pg} and P_{sg} at 0 °C and E_{Lp} and E_{Ps}) together with L_p and P_s at 4, 15 and 25 °C are presented in Figure 4C–D. There is no significant difference among most of the L_p or P_s values at each of the different temperatures. No CPA dependence was observed for either L_p or P_s and both L_p and P_s increase with increasing temperature. The four coefficients L_{pg}, P_{sg}, E_{Lp}, and E_{Ps} obtained from the Arrhenius plot are also listed in Table 1 along with their values reported in the literature.[41, 42, 44–46] The activation energies for water transport across the cell plasma membrane in the presence of the three CPAs follows: $E_{Lp}^{PG} > E_{Lp}^{EG} > E_{Lp}^{Trehalose}$ and the activation energy for the transport of PG (E_{Ps}^{PG}) is greater than that of EG (E_{Ps}^{EG}). This implies that the temperature dependence of the permeability coefficient is the strongest in the presence of PG, followed by EG and trehalose. The presence of membrane-penetrating CPAs (EG or PG) appears to slightly decrease water transport across the cell membrane at low temperatures ($T<15^{\circ}\mathrm{C}$), while it is reversed at high temperatures ($T \geq 15^{\circ}\mathrm{C}$). This effect is more pronounced for PG than EG (Figure 4C). These data may be valuable for the design or optimization of CPA addition/removal protocols.

The Arrhenius plots of both the data obtained in this study and available data from several previous works[25, 27, 41–44, 46] (also listed in Table S3, supplementary information) are shown in Figure 4E. Our results are consistent with the literature. Thus, we are confident that the current work provides a feasible and reliable approach to the quantitative description of the transport properties of the cell membrane of human oocyte.

Fertilization and developmental competence analysis post perfusion

To confirm the procedure used in this study does not compromise the physiological function of *in-vitro* matured human oocytes, insemination of the oocytes after perfusion in the microfluidic device was performed using intracytoplasmic sperm injection (ICSI, Figure 5A). Fertilized oocytes (indicated by the appearance of 2-pronuclei, 2PN) were cultured for both fresh (control) and the perfused groups. Phase contrast micrographs showing the morphology of the oocytes before fertilization, fertilized oocytes at the 2PN stage, and the 4-cell stage embryos are given in Figure 5B. No visible difference was observed in terms of the morphology and development competence between the two groups. As shown in Figure S4 (Supplementary Information), there was no significant difference in fertilization and cleavage rates between the fresh and perfused groups (for the same CPA, data from the three different temperatures were piled up for this comparison). This is attributed to the gradual increase in the osmolality (Figure 2A–C) around the oocytes in the microchannel while the commonly used method to increase the osmolality around the oocytes stepwise by manual pipetting may cause osmotic shock/injury to the cells.[3] It is worth noting that even much

reduced shrinkage rate (for cells that are much more sensitive to osmotic shock) could be achieved by adjusting the flow rate of the perfusion fluids to eliminate osmotic injury to cells without compromising the effectiveness of the approach to determine the transport properties.

Features of the microfluidic approach

Several conventional methods, such as direct microscopic observation[2, 23–25], microscope diffusion chamber,[26, 27] microperfusion chamber,[28] and micropipette perfusion[20–22], have been developed for measuring the oocyte membrane transport properties.

For both the direct microscopic observation and micropipette perfusion methods, the oocyte is suddenly exposed to the non-isotonic solutions, which may incur osmotic injury to the cell.[3] In addition, the uncontrolled mixing of extracellular solutions may be difficult to analyze theoretically, which may compromise the accuracy of calculating the transport properties. Similarly, for both the microscope diffusion chamber and the microperfusion chamber approaches,[26–28] the introduction of a dialysis or transparent porous membrane increases the mathematical complexity for modeling extracellular mixing to accurately calculate the transport properties. In addition, the complexity of assembling the chambers is a hurdle to the widespread use of the two chamber-based approaches. In contrast, the microfluidic device that we developed is more controllable in terms of extracellular mixing and it is easy and fast to assemble with high precision.

Compared with existing microfluidic devices for investigation of oocyte membrane transport properties,[3, 18] our approach does not require specialized facilities such as the clean room for fabrication of the mold for soft lithography and a plasma oven for bonding. Moreover, our device allows long-term or repeated use, which may not be achievable with the published PDMS microfluidic devices.[32–35] As a result, our device offers the unique features of being cost effective, robust, reusable, and durable.

More importantly, both the theoretically rigorous analysis of the mixing in the microchannel and the direct cell scale measurement of the temperature of the extracellular solution may greatly enhance the accuracy of determining the transport properties. Owing to the capacity of excellent control of both solution replacement and temperature (similar to the microfluidic device for oocyte culturing[68, 69]), the proposed microfluidic device might also be used as a novel platform for in vitro culture of immature or fertilized human oocytes.

Conclusions

In conclusion, a novel microfluidic perfusion approach for on-chip characterization of the transport properties of *in-vitro* matured human oocytes is developed. This approach enables determination of the membrane transport properties of cells under minimal osmotic shock or injury to the cells. Its cost-effectiveness, ease of fabrication, long-term durability, and robustness make the microfluidic perfusion system a powerful tool for studying the membrane transport properties with applications in reproductive pharmacology, fertility preservation, and assisted reproduction.

Supplementary Material

Refer to Web version on PubMed Central for supplementary material.

Acknowledgments

This work was partially supported by grants from NSFC (Nos. 51476160, 51528601 and 11627803) to GZ. ZZ was supported by the Natural Science Foundation of Anhui Provincial Universities (KJ2014A114). XH was supported by grants from NIH (R01EB012108 and R01EB023632).

References

1. McGrath JJ. Cryobiology. 1997; 34:315–334. [PubMed: 9200819]
2. Han X. Cryoletters. 2016; 37:394–400. [PubMed: 28072425]
3. Lai D, Ding J, Smith GW, Smith GD, Takayama S. Human reproduction. 2015; 30:37–45. [PubMed: 25355589]
4. Yu L, Peterson B, Inhorn MC, Boehm JK, Patrizio P. Human reproduction. 2016; 31:403–411. [PubMed: 26677956]
5. Abir R, Ben-Aharon I, Garor R, Yaniv I, Ash S, Stemmer SM, Ben-Haroush A, Freud E, Kravarusic D, Sapir O, Fisch B. Human reproduction. 2016; 31:750–762. [PubMed: 26848188]
6. Konc J, Kanyo K, Kriston R, Somoskoi B, Cseh S. BioMed research international. 2014; 2014:307268. [PubMed: 24779007]
7. Clark NA, Swain JE. Journal of assisted reproduction and genetics. 2013; 30:865–875. [PubMed: 23779099]
8. Paynter SJ. Human reproduction update. 2000; 6:449–456. [PubMed: 11045876]
9. Borini A, Sciajno R, Bianchi V, Sereni E, Flamigni C, Coticchio G. Human reproduction. 2006; 21:512–517. [PubMed: 16239316]
10. Tsai S, Yen W, Chavanich S, Viyakarn V, Lin C. PLoS One. 2015; 10:e0123409. [PubMed: 26010144]
11. Tan YJ, Zhang XY, Ding GL, Li R, Wang L, Jin L, Lin XH, Gao L, Sheng JZ, Huang HF. Sci Rep. 2015; 5:17741. [PubMed: 26634435]
12. Schiewe MC, Zozula S, Anderson RE, Fahy GM. Cryobiology. 2015; 71:264–272. [PubMed: 26210008]
13. Jin B, Mazur P. Sci Rep. 2015; 5:9271. [PubMed: 25786677]
14. Mazur P. J Gen Physiol. 1963; 47:347. [PubMed: 14085017]
15. Zhao G, Fu J. Biotechnol Adv. 2017; doi: 10.1016/j.biotechadv.2017.01.006
16. Steltenkamp S, Rommel C, Wegener J, Janshoff A. Small. 2006; 2:1016–1020. [PubMed: 17193161]
17. Park S, Wijethunga PA, Moon H, Han B. Lab on a chip. 2011; 11:2212–2221. [PubMed: 21603697]
18. Heo YS, Lee HJ, Hassell BA, Irimia D, Toth TL, Elmoazzen H, Toner M. Lab Chip. 2011; 11:3530–3537. [PubMed: 21887438]
19. Song YS, Moon S, Hulli L, Hasan SK, Kayaalp E, Demirci U. Lab Chip. 2009; 9:1874–1881. [PubMed: 19532962]
20. Gao DY, McGrath JJ, Tao J, Benson CT, Critser ES, Critser JK. J Reprod Fertil. 1994; 102:385–392. [PubMed: 7861392]
21. Karlsson JO, Younis AI, Chan AW, Gould KG, Eroglu A. Mol Reprod Dev. 2009; 76:321–333. [PubMed: 18932214]
22. De Santis L, Coticchio G, Paynter S, Albertini D, Hutt K, Cino I, Iaccarino M, Gambardella A, Flamigni C, Borini A. Human reproduction. 2007; 22:2776–2783. [PubMed: 17675355]
23. Leibo SP. J Membrane Biol. 1980; 53:179–188. [PubMed: 7190193]
24. Wang X, Al Naib A, Sun DW, Lonergan P. Cryobiology. 2010; 61:58–65. [PubMed: 20470768]

25. Newton H, Pegg DE, Barrass R, Gosden RG. J Reprod Fertil. 1999; 117:27–33. [PubMed: 10645242]
26. McGrath JJ. Journal of microscopy. 1985; 139:249–263. [PubMed: 4078888]
27. Bernard A, McGrath JJ, Fuller BJ, Imoedemhe D, Shaw RW. Cryobiology. 1988; 25:495–501. [PubMed: 3234012]
28. Gao DY, Benson CT, Liu C, McGrath JJ, Critser ES, Critser JK. Biophys J. 1996; 71:443–450. [PubMed: 8804627]
29. Zhao, G., Huang, ZP., Gao, DY. Multiscale Technologies for Cryomedicine. He, XM., Bischof, JC., editors. World Scientific Publishing Co Pte Ltd; 2016.
30. Lyu SR, Chen WJ, Hsieh WH. Sensors and Actuators B: Chemical. 2014; 197:28–34.
31. Lai D, Takayama S, Smith GD. Journal of biomechanics. 2015; 48:1671–1678. [PubMed: 25801423]
32. Suchy T, Sedlacek R, Sucharda Z, Balik K, Bouda T. Comput Method Biomec. 2013; 16:255–257.
33. Kim M, Moon BU, Hidrovo CH. J Micromech Microeng. 2013; 23
34. Xiang KW, Huang GS, Zheng J, Wang XA, Li GX, Huang JY. J Polym Res. 2012; 19
35. McCarthy DW, Mark JE. Rubber Chemistry and Technology. 1998; 71:906–927.
36. Takamatsu H, Komori Y, Zawlodzka S, Fujii M. J Biomech Eng-T Asme. 2004; 126:402–409.
37. Zhang ZG, Zhao JH, Wei ZL, Cong L, Zhou P, Cao YX. Archives of andrology. 2007; 53:303–307. [PubMed: 18357959]
38. Zhang Z, Liu Y, Xing Q, Zhou P, Cao Y. Reproductive biology and endocrinology : RB&E. 2011; 9:156. [PubMed: 22151887]
39. Huang HS, Choi JK, Rao W, Zhao ST, Agarwal P, Zhao G, He XM. Advanced Functional Materials. 2015; 25:6839–6850.
40. Wang JY, Zhao G, Zhang ZL, Xu XL, He XM. Acta Biomaterialia. 2016; 33:264–274. [PubMed: 26802443]
41. Van den Abbeel E, Schneider U, Liu J, Agca Y, Critser JK, Van Steirteghem A. Human reproduction. 2007; 22:1959–1972. [PubMed: 17428880]
42. Paynter SJ, O'Neil L, Fuller BJ, Shaw RW. Fertility and sterility. 2001; 75:532–538. [PubMed: 11239537]
43. Mullen SF, Li M, Li Y, Chen ZJ, Critser JK. Fertility and sterility. 2008; 89:1812–1825. [PubMed: 17681308]
44. Paynter SJ, Cooper A, Gregory L, Fuller BJ, Shaw RW. Human reproduction. 1999; 14:2338–2342. [PubMed: 10469706]
45. Hunter J, Bernard A, Fuller B, McGrath J, Shaw R. Cryobiology. 1992; 29:240–249. [PubMed: 1582230]
46. Hunter J, Bernard A, Fuller B, McGrath J, Shaw R. Journal of cellular physiology. 1992; 150:175–179. [PubMed: 1730781]
47. Shu Z, Hughes SM, Fang C, Hou Z, Zhao G, Fialkow M, Lentz G, Hladik F, Gao D. Biopreserv Biobank. 2016; 14:307–313. [PubMed: 26977578]
48. Yue C, Zhao G, Yi JR, Gao C, Shen LX, Zhang YT, Wang Z, Liu W. Cryobiology. 2014; 69:273–280. [PubMed: 25111088]
49. Agca Y, Liu J, McGrath JJ, Peter AT, Critser ES, Critser JK. Cryobiology. 1998; 36:287–300. [PubMed: 9654733]
50. Liu J, Zieger MAJ, Lakey JRT, Woods EJ, Critser JK. Cryobiology. 1997; 35:1–13. [PubMed: 9245505]
51. Woods E, Liu J, Gilmore J, Reid T, Gao D, Critser J. Cryobiology. 1999; 38:200–208. [PubMed: 10328910]
52. Benson C, Liu C, Gao D, Critser E, Benson J, Critser J. Cryobiology. 1998; 37:290–299. [PubMed: 9917345]
53. Wang MH, Soriano AN, Caparanga AR, Li MH. J Taiwan Inst Chem E. 2010; 41:279–285.
54. FernandezSempere J, RuizBevia F, ColomValiente J, MasPerez F. J Chem Eng Data. 1996; 41:47–48.

55. Ternstrom G, Sjostrand A, Aly G, Jernqvist A. J Chem Eng Data. 1996; 41:876–879.
56. Ekdawi-Sever N, de Pablo JJ, Feick E, von Meerwall E. J Phys Chem A. 2003; 107:936–943.
57. Kvon A, Lee YH, Cheema TA, Park CW. Measurement Science and Technology. 2014; 25
58. Roman S, Lorthois S, Duru P, Risso F. Microvascular Research. 2012; 84:249–261. [PubMed: 22963788]
59. Kleinhans FW. Cryobiology. 1998; 37:271–289. [PubMed: 9917344]
60. Katkov II. Cryobiology. 2000; 40:64–83. [PubMed: 10679151]
61. Zhang SZ, Chen GM. Cryobiology. 2002; 44:204–209. [PubMed: 12237085]
62. Chuenkhum S, Cui ZF. Cryoletters. 2006; 27:185–199. [PubMed: 16892167]
63. Ren J, Zhao G. Cryoletters. 2013; 34:404–412. [PubMed: 23995408]
64. Zhurova M, McGann LE, Acker JP. Cryobiology. 2014; 68:379–388. [PubMed: 24727610]
65. Zhao G. Cryoletters. 2010; 31:279–290. [PubMed: 20919457]
66. Mazur P, Cacheiro LH. Cryobiology. 1977; 14:681–681.
67. Niu D, Zhao G, Liu X, Zhou P, Cao Y. Tissue engineering Part C, Methods. 2016; 22:270–279. [PubMed: 26701745]
68. Swain JE, Lai D, Takayama S, Smith GD. Lab Chip. 2013; 13:1213–1224. [PubMed: 23400523]
69. Han C, Zhang QF, Ma R, Xie L, Qiu TA, Wang L, Mitchelson K, Wang JD, Huang GL, Qiao J, Cheng J. Lab Chip. 2010; 10:2848–2854. [PubMed: 20844784]

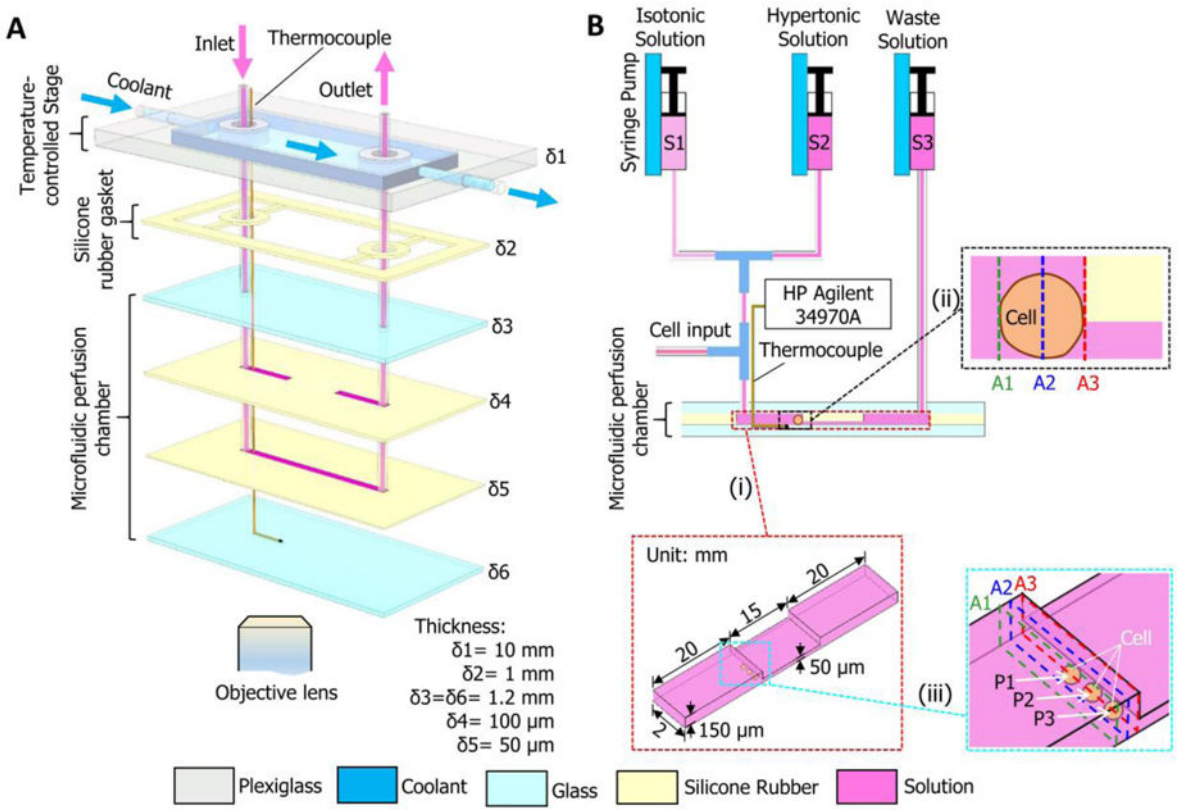

Figure 1.

A schematic illustration of the microfluidic perfusion system. (A) An expanded view showing the configuration of the microdevice with a microfluidic perfusion chamber and an integrated temperature-controlled stage. (B) A diagram showing the connections between the microdevice and three syringes and the microchannels. Arrows indicate the direction of fluid flow. The HP Agilent 34970A data acquisition system is for monitoring and recording temperature with the thermocouple. δ1–δ6, thickness; S1–S3, syringes; A1–A3, representative cross sections; P1–P3, typical cell locations. Note: drawing not to scale.

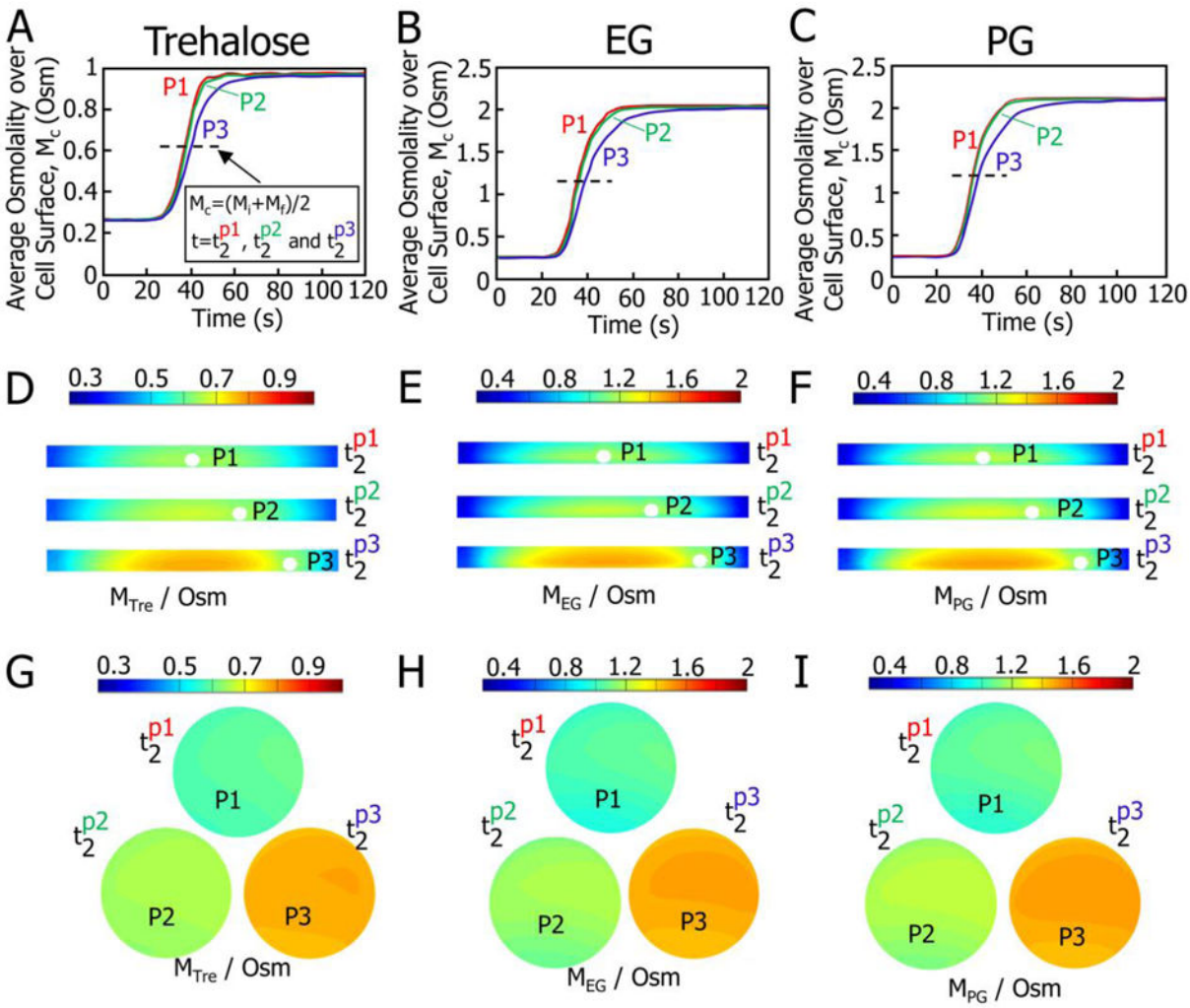

Figure 2.

Predicted osmolality over the surface of a cell located at P1–P3 and in the solutions in the microchannel after introducing the hypertonic solution made by dissolving 0.56 M trehalose, 1.5 M EG, and 1.5 M PG in an isotonic solution (Quinn's Advantage medium supplemented with HEPES and 10% v/v serum substitute supplement). (A–C) Integral-averaged osmolality profiles over cell surface. (D–F) Transient osmolality distributions for cross-section A2 at the different values of characteristic time t_2 for P1–P3. (G–I) Transient osmolality distributions over the cell surface at the different values of characteristic time t_2. The t_2 corresponds to the time when the integral-averaged osmolality M_c climbs up to the average of the initial (M_i) and the final (M_f) values, $M_c=(M_i+M_f)/2$. The t_2 for P1, P2 and P3 is different and represented by t_2^{p1}, t_2^{p2} and t_2^{p3}, respectively.

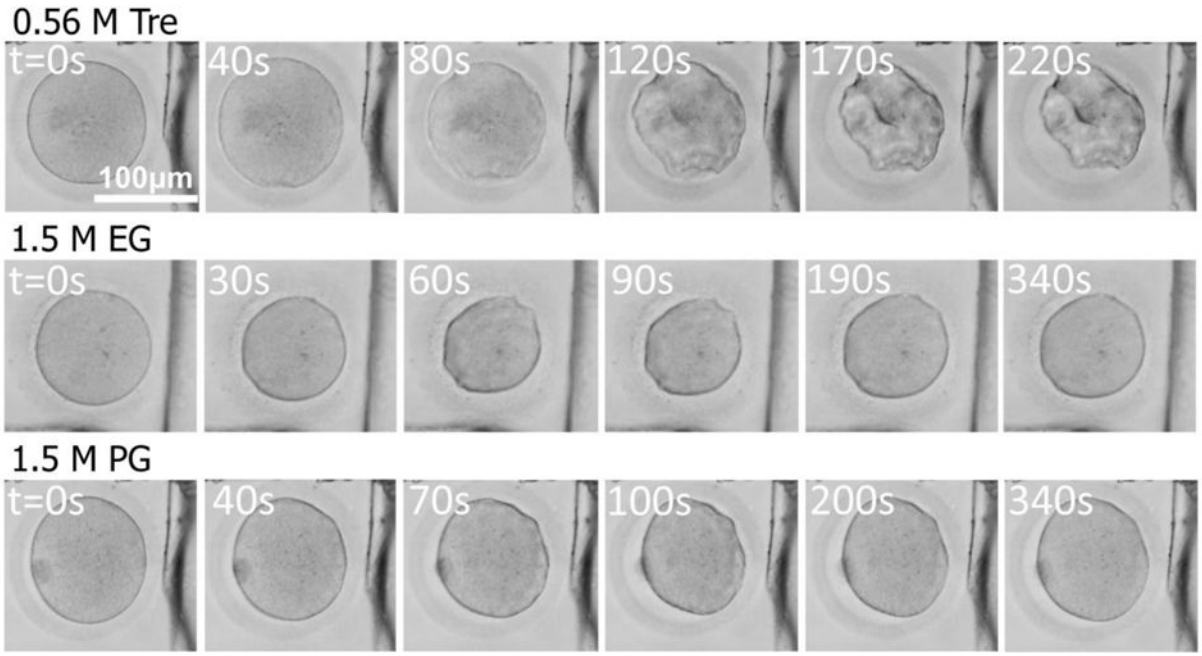

Figure 3.

Typical photomicrographs of *in vitro* matured human oocytes (at P1) showing volume responses of the cells after exposed to hypertonic solutions (0.56 M trehalose, 1.5 M EG and 1.5 M PG in cell culture medium) at 25 °C.

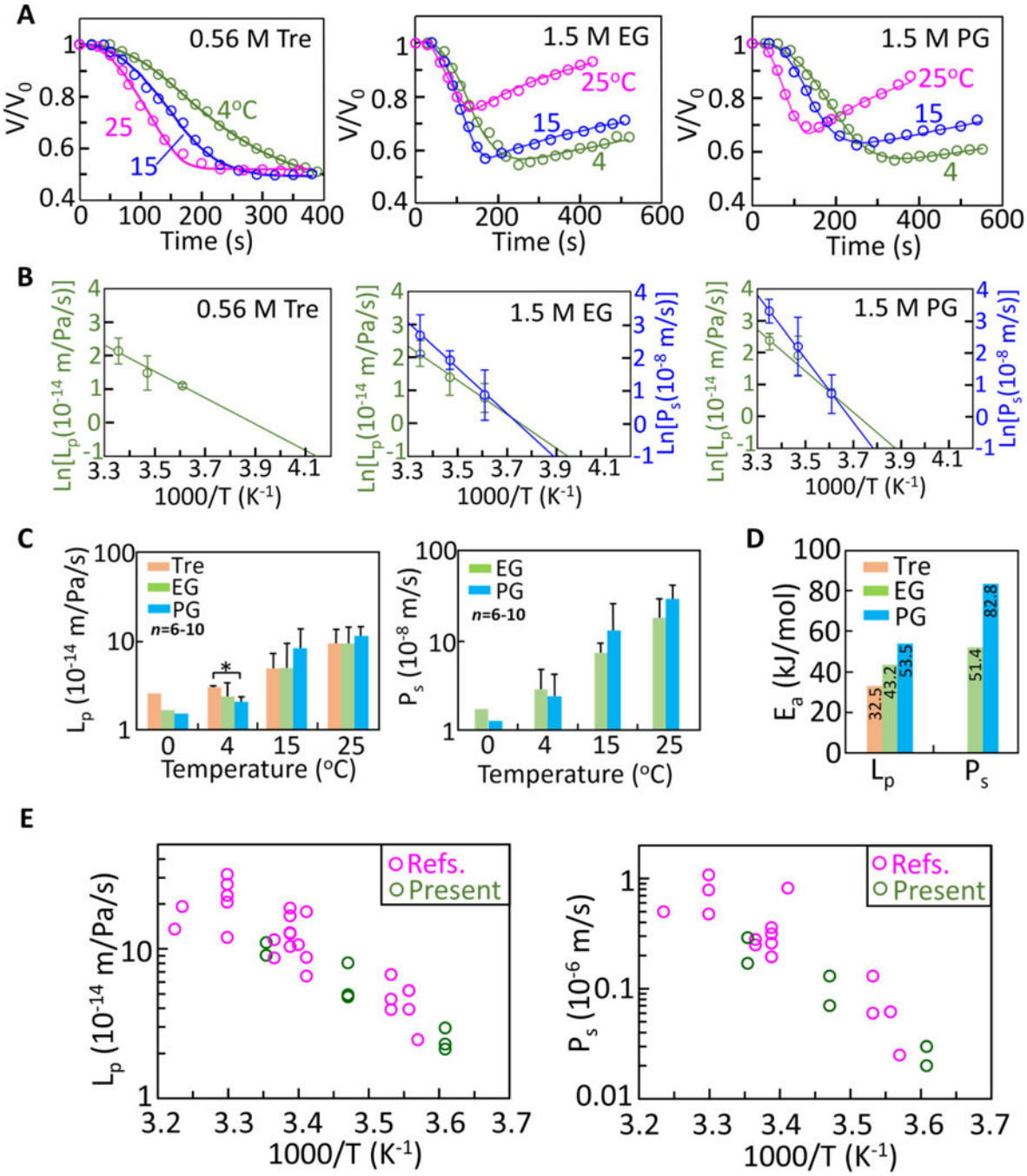

Figure 4.

Transport properties of human *in-vitro* matured oocytes. (A) Cell volume responses upon introduction of 0.56 M trehalose, 1.5 M EG, and 1.5 M PG at 4, 15, and 25 °C and the corresponding curve fitting results (lines) with the 2-*p* model of water/solute transport. (B) Arrhenius plots of the temperature-dependent membrane permeability coefficients (L_p and P_s). (C) The L_{pg} and P_{sg} (i.e., the reference values for L_p and P_s at 0 °C, respectively) together with L_p and P_s at 4, 15, and 25 °C. (D) The activation energies for water and CPA (EG and PG) transport across the cell membrane. (E) The membrane permeability

coefficients (L_p and P_s) and their temperature dependence determined by this study together with those reported in the literature[25, 27, 41–46].

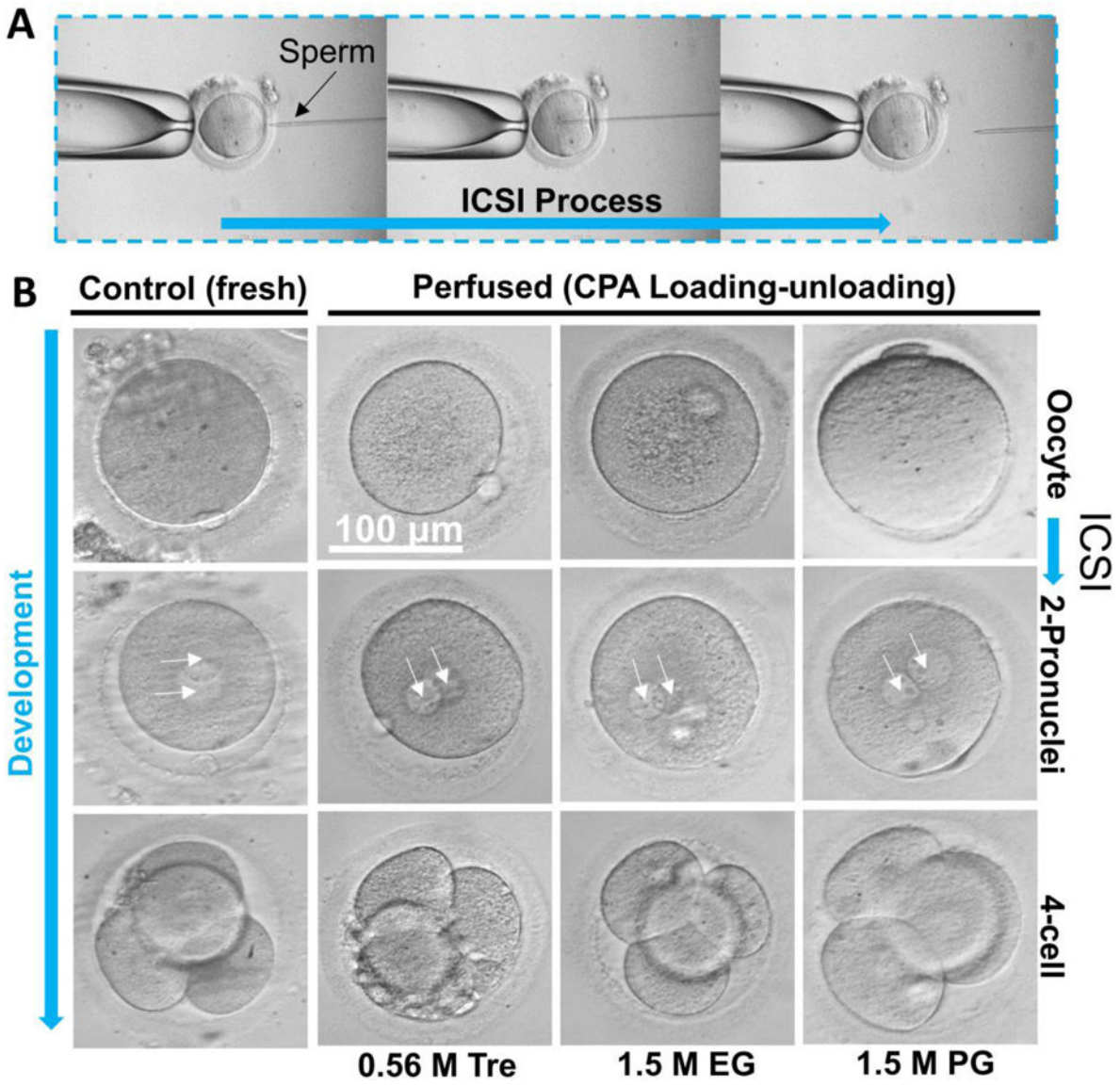

Figure 5.

Fertilization of human *in-vitro* matured oocytes for both the fresh (control) and the perfused (subjected to a CPA addition-removal cycle) groups by intracytoplasmic sperm injection (ICSI, A) and photomicrographs (B) showing the morphology of the oocytes before fertilization and 2-pronuclei (2PN) and 4-cell embryos developed from the fertilized oocytes.

Table 1

Transport properties of *in-vitro* matured human oocytes

CPA (mol/L)	L_{pg}	E_{Lp}	P_{sg}	E_{ps}	T	Ref.
	10^{-14} m/Pa/s (μm/atm/min)	kJ/mol (kcal/mol)	10^{-8} m/s (μm/min)	kJ/mol (kcal/mol)	°C	
Trehalose (0.56)	2.45 (0.15)	32.49 (7.76)	–	–	4, 15, 25	present
EG (1.5)	1.63 (0.09)	43.21 (10.32)	1.77 (1.06)	51.44 (12.29)		
PG (1.5)	1.51 (0.09)	53.52 (12.79)	1.26 (0.76)	82.76 (19.77)		
DMSO (1.5)	1.70 (0.10)	61.14 (14.61)	1.41 (0.85)	89.63 (21.41)	10, 24, 30	[44]
Galactose (0.9)	2.13 (0.13)	57.06 (13.63)	–	–	8, 22, 30	[41]
EG (1.5)	2.88 (0.18)	46.84 (11.19)	2.54 (1.52)	66.17 (15.81)		
PG (1.5)	2.80 (0.17)	52.28 (12.49)	3.93 (2.36)	72.74 (17.38)	10, 24, 30	[42]
NaCl (0.5)	5.40 (0.33)	10.20 (2.44)	–	–	10, 20, 30, 37	[45]
NaCl (0.5)	2.45 (0.15)	34.92 (8.34)	–	–	10, 20, 30, 37	[46]